

# A new look at the deconfinement transition with parallel tempering

Szabolcs Borsanyi

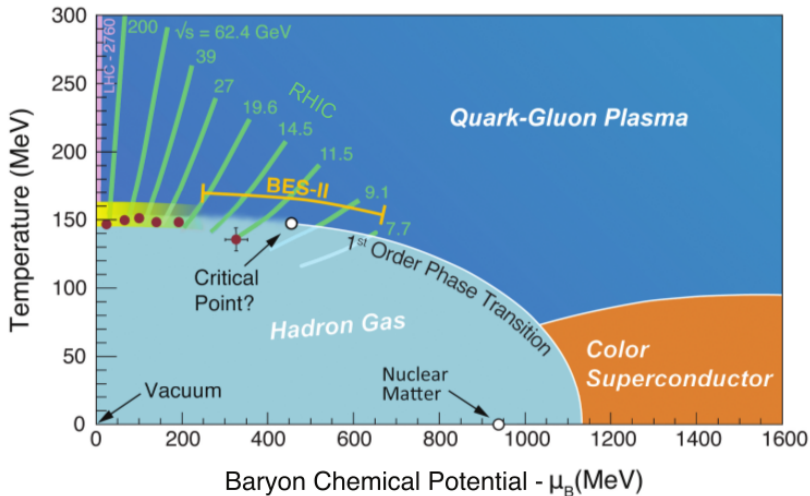
University of Wuppertal

ECT\*, Trento, May 25, 2022

Gauge Topology, Flux Tubes and Holographic Models



# Beam energy scan program



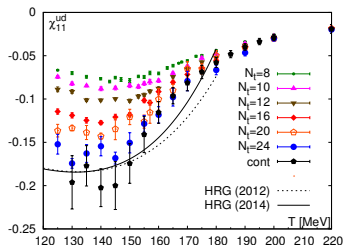
BES-II: chemical potentials of interest:  $\mu_B/T = 1.5 \dots 4$

# How strong is the sign problem?

The complex phase of the fermion determinant is linked to a physical observable, the light quark density. [[See formula 5.2 of Allton et al hep-lat/0501030]]

$$\det M = |\det M| e^{i\theta} \quad \theta = \frac{1}{4} N_f \text{Im} \left[ \mu \underbrace{\frac{\partial \ln \det M}{\partial \mu}}_{\text{light quark density}} + \dots \right]$$

$$\langle \theta^2 \rangle = -\frac{1}{9} \mu_B^2 L^3 T N_f^2 \chi_{11}^{ud} \quad \text{with} \quad \chi_{11}^{ud} \sim \partial^2 \log Z / \partial \mu_u \partial \mu_d .$$



*The sign problem is weak for coarse lattices and at high temperatures.*

# Sign problem in the practice

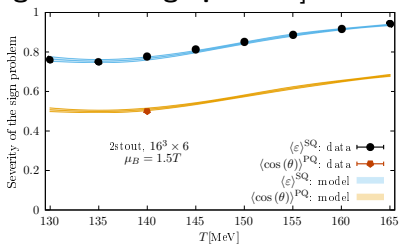
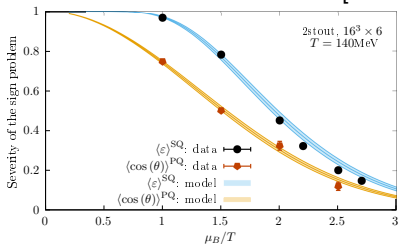
Idea: *sign quenched simulations*:  $\text{Re} e^{i\theta} = \underbrace{\pm}_{\text{reweighting}} \underbrace{|\cos(\theta)|}_{\text{simulation}}$

[Budapest 2004.10800]

For a concrete case:

- 2-stout-staggered action,
- physical quarks with 2+1 flavors,
- $16^3 \times 6$  lattice.

Statistics required  $\sim \frac{1}{[\text{Strength of the sign problem}]^2}$



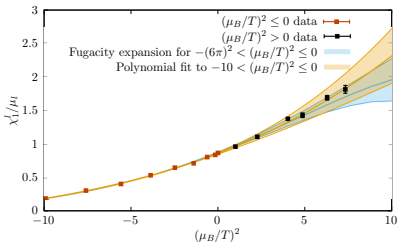
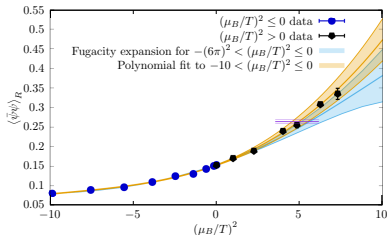
*The data points are actual simulations!*

[Wuppertal-Budapest 2108.09213]

## How far can we go in the chemical potential?

We compare in these plots for 140 MeV

- Taylor expansion from imaginary  $\mu_B$
- Fugacity expansion from imaginary  $\mu_B$
- Direct finite density simulations at  $0 < \mu_B \leq 380$  MeV



The direct result has the smallest errors.

Simulation in two steps:

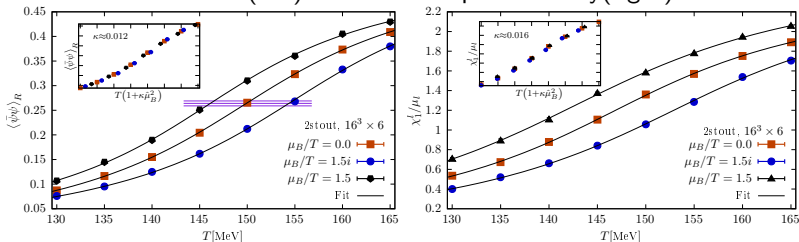
- 1 Simulate the real (sign quenched) action
- 2 Reweight each configuration with the correct sign

**Feasible as long as the sign problem is not too severe.**

*The earlier, tighter constraint of the overlap problem was removed.*

Drawback: the simulation algorithm is more expensive (*subject to research*)

The chiral condensate (left) and the real quark density (right).

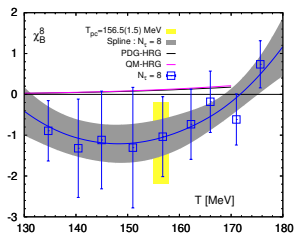
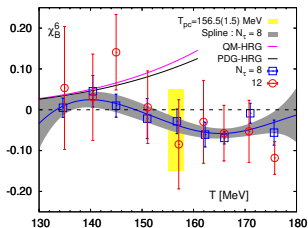


*The plots show the matching imaginary  $\mu_B$  results for comparison.*

Inset plots: the scaling with temperature survives to real  $\mu_B$  !

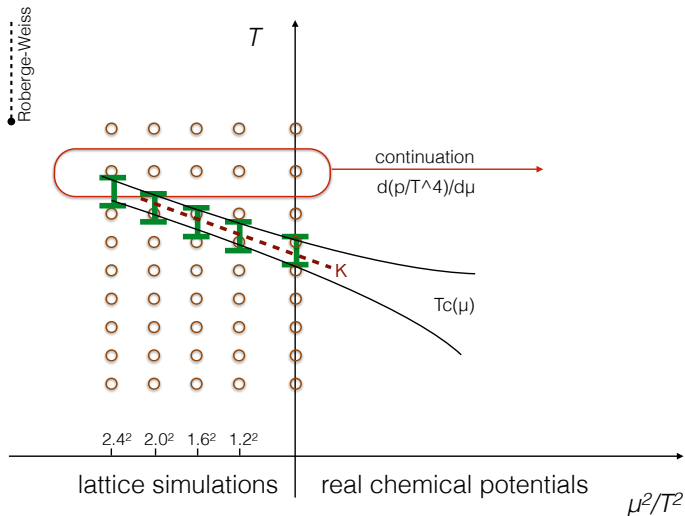
$$\frac{p}{T^4} = \sum_{n=0}^{\infty} \frac{1}{n!} \frac{\partial^n p / T^4}{(\partial \mu_B)^n} = \sum_{n=0}^{\infty} \frac{1}{n!} \chi_B^n$$

Sixth and eighth order baryon fluctuations =  $\mathcal{O}(\mu_B^6)$  and  $\mathcal{O}(\mu_B^8)$  coefficients



| $N_\tau = 8$ |           | $N_\tau = 12$ |         |
|--------------|-----------|---------------|---------|
| T [MeV]      | #conf.    | T [MeV]       | #conf.  |
| 134.64       | 1,275,380 | 134.94        | 256,392 |
| 140.45       | 1,598,555 | 140.44        | 368,491 |
| 144.95       | 1,559,003 | 144.97        | 344,010 |
| 151.00       | 1,286,603 | 151.10        | 308,680 |
| 156.78       | 1,602,684 | 157.13        | 299,029 |
| 162.25       | 1,437,436 | 161.94        | 214,671 |
| 165.98       | 1,186,523 | 165.91        | 156,111 |
| 171.02       | 373,644   | 170.77        | 144,633 |
| 175.64       | 294,311   | 175.77        | 131,248 |

# Analytic continuation



Many exploratory studies: [de Forcrand & Philipsen hep-lat/0205016]

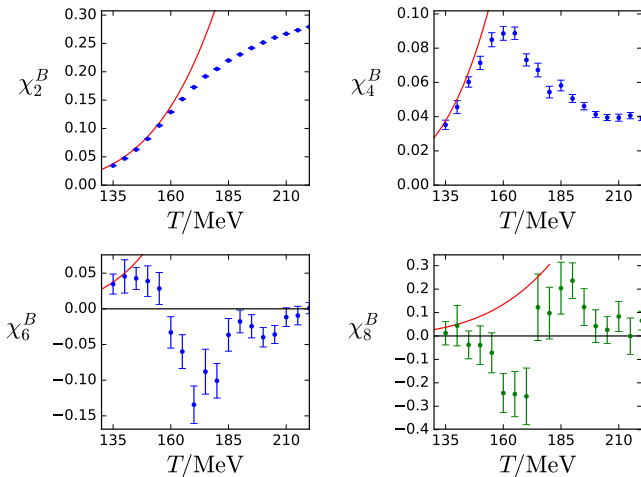
[Philipsen 0708.1293] [Philipsen 1402.0838] [Cea et al hep-lat/0612018,0905.1292,1202.5700]

[Wuppertal 1607.02493] [D'Elia et al 1611.08285]



# Higher order $\chi_B$ from imaginary $\mu_B$

“Numerical derivatives” from  $\mu_B^2 \leq 0$  simulations: [\[WB 1805.04445\]](#)

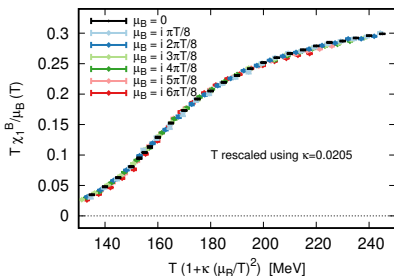
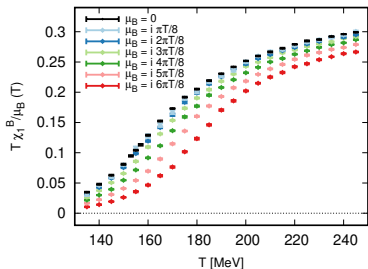


This structure is already known from chiral effective models. [\[Friman et al 1103.3511\]](#)

*There is a rather simple model that quantitatively describes the  $\chi$  coefficients.*

# Observations at imaginary $\mu_B$

Normalized baryon density:  $\chi_1^B(T, \hat{\mu}_B)/\mu_B = n_B/\mu_B$



From simulations at imaginary  $\mu_B$  we observe that  $\chi_1^B(T, \hat{\mu}_B)$  is to good approximation:

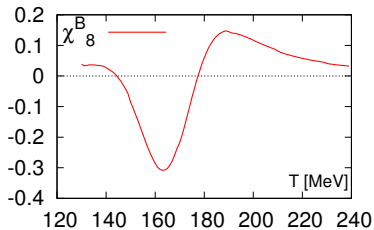
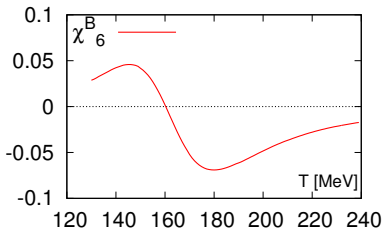
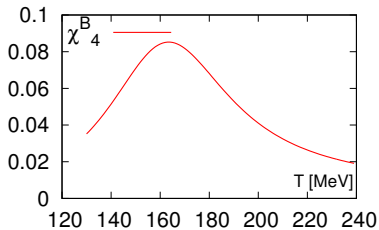
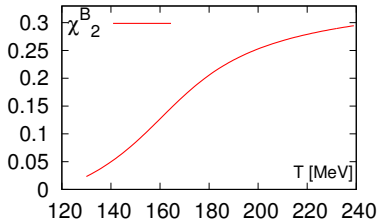
$$\chi_1^B(T, \hat{\mu}_B) = \mu_B \chi_2^B(T(1 + \kappa \hat{\mu}_B^2), 0)$$

Expand both sides in  $\mu_B$ :

$$\hat{\mu}_B \chi_2^B(T, 0) + \frac{\hat{\mu}_B^3}{6} \chi_4^B(T, 0) + \dots = \mu_B \chi_2^B(T, 0) + \mu_B^3 T \kappa \frac{d\chi_2^B(T, 0)}{dT} + \dots$$

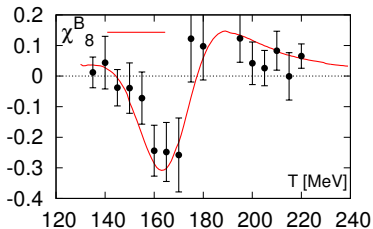
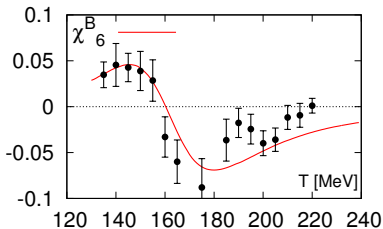
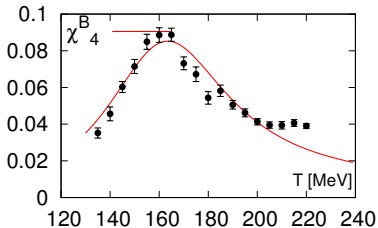
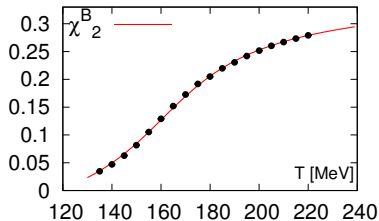
# Higher order $\chi_B$ in the simple model

Input:  $\chi_2^B(T, \mu = 0)$  from Wuppertal-Budapest, and  $\kappa = 0.02$  [see 1508.07599]:



# Higher order $\chi_B$ in the simple model

Comparing the simple model with our lattice result:



Simple model describes lattice result surprisingly well.

*Result is consistent with the no-critical-end-point scenario.*

# Expansion scheme: formal definition

Our naive observation (almost correct):

$$\chi_1^B(T, \hat{\mu}_B) = \hat{\mu}_B \chi_2^B(T \cdot (1 + \kappa_2 \hat{\mu}_B^2), 0)$$

Let's generalize this to endorse any sigmoid  $\chi_1^B(T, \hat{\mu}_B)$  result:

$$\chi_1^B(T, \hat{\mu}_B) = \hat{\mu}_B \cdot \chi_2^B [T \cdot (1 + \kappa_2(T) \cdot \hat{\mu}_B^2 + \kappa_4(T) \cdot \hat{\mu}_B^4 + \dots)]$$

The **complete finite density equation of state** is then contained in

- $\chi_2^B(T)$ : baryon number susceptibility (known precisely)
- $\kappa_2(T), \kappa_4(T)$  a series of slowly varying functions

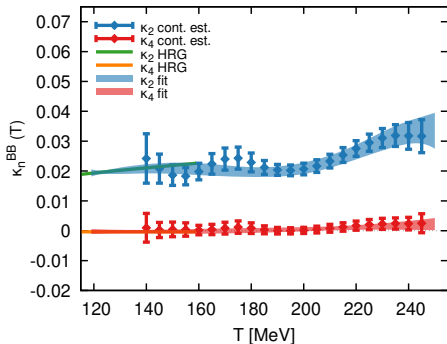
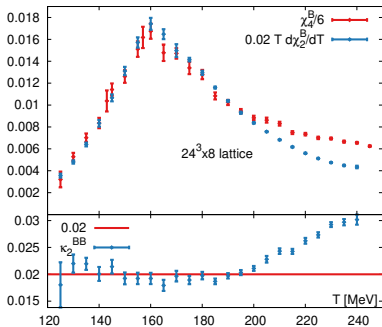
*These functions are directly related to the Taylor coefficients:*

$$\kappa_2(T) = \frac{1}{6T} \frac{\chi_4^B(T)}{\chi_2^{B'}(T)}$$

$$\kappa_4(T) = \frac{1}{360 \chi_2^{B'}(T)^3} \left( 3 \chi_2^{B'}(T)^2 \chi_6^B(T) - 5 \chi_2^{B''}(T) \chi_4^B(T)^2 \right)$$

# The results for $\kappa_2(T)$ , $\kappa_4(T)$

Fairly constant  $\kappa_2(T)$  over a large  $T$ -range,  $\kappa_4(T)$  is less by an order of magnitude.



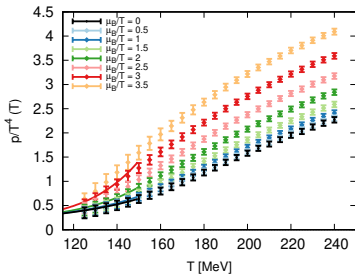
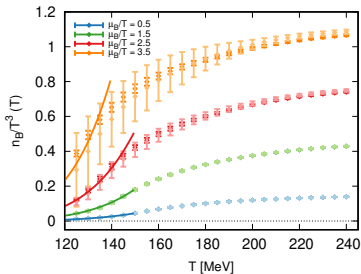
$$\kappa_2(T) T \frac{d\chi_2^B}{dT} = \chi_4^B(T)/6$$

[Wuppertal Budapest 2102.06660]

# Thermodynamics at finite (real) $\mu_B$

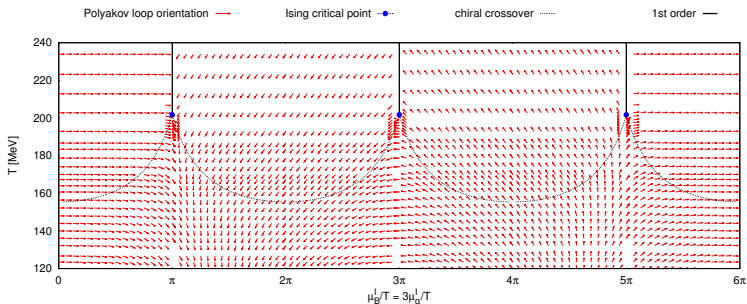
baryon density and pressure

- We reconstruct thermodynamic quantities up to  $\hat{\mu}_B \simeq 3.5$  with uncertainties well under control
- Agreement with HRG model calculations at small temperatures
- No pathological (non-monotonic) behavior is present



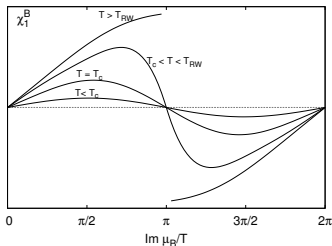
[Wuppertal Budapest 2102.06660 ]

# Phase diagram at imaginary baryo-chemical potential:



[Fodor & Katz hep-lat/0104001] [de Forcrand & Philipsen hep-lat/0205016] [D'Elia & Lombardo hep-lat/0209146]

[D'Elia et al 0705.3814] [Philipsen 0708.1293, 1402.0838] [Cea et al hep-lat/0612018,0905.1292,1202.5700] [Bonati et al 1602.01426]



At low  $T$  only  $B$  states contribute:

$$\chi_1^B \sim \sin(\mu_B/T)$$

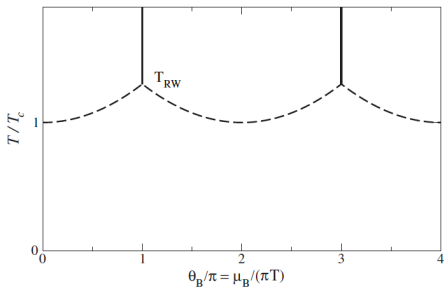
At high  $T$  fractional charges are required to make a first order transition at  $\mu_B = \pi T$ :

$$\chi_1^B \sim \sin(\mu_B/T/3)$$

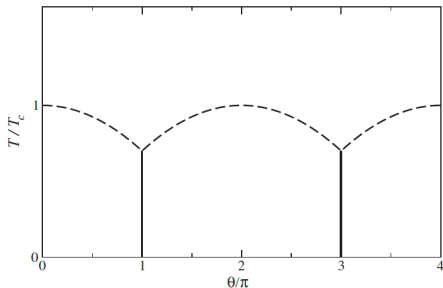


# Analogous phase diagrams $\text{Im}\mu_B - T$ vs. $\Theta - T$

MASSIMO D'ELIA AND FRANCESCO NEGRO



PHYSICAL REVIEW D **88**, 034503 (2013)

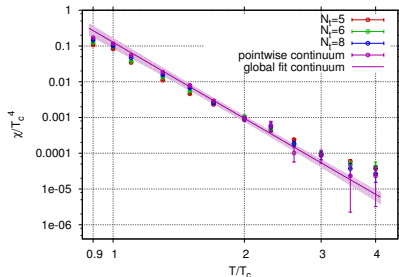
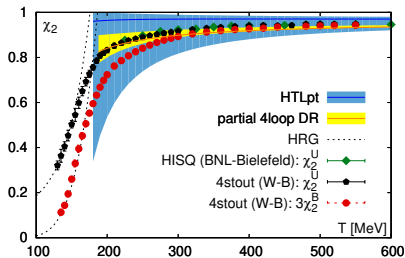


- Periodicity: integer baryon number and topological charge
- Suppressed fluctuations  
 *$\mu_B$ : heavy hadrons  $T < T_c$  ;  $\theta$ : dilute instantons [Yaffe&Gross (1981)]*
- 1st order transition:  
 *$\mu_B$ : weak coupling  $T > T_c$  ;  $\theta$ :  $\chi \sim N^0$  in large- $N$   $T > T_c$  [Witten (1998)]*
- Sign problem on the lattice for real  $\mu_B$  and real  $\theta$
- 2nd  $\mu_B$  or  $\theta$  derivative: susceptibilities  $\chi(T)$

# Baryon fluctuations vs. topological susceptibility

- Left:  $\chi_B(T)$ , baryon fluctuations are suppressed by a Boltzmann factor at low  $T$ , high  $T$ : Stefan-Boltzmann limit
- Right:  $\chi_t(T)$ , topological fluctuations are suppressed at high  $T$ :

$$\chi(T) \sim T^4 e^{-2\pi/\alpha_s} \sim T^{4-11} \sim T^{-7} \sim T^{-b}$$



$N_f = 0$ ,  $\chi_t$  lattice data: [Wuppertal 1508.06917]

$N_f = 2 + 1 + 1$ ,  $\chi_B$  lattice data: [Wuppertal 1507.04627]

# Many methodical improvements to lattice $\chi_t(T)$

- Simulations at imaginary  $\theta$

[Panagopoulos&Vicari 1109.6815]

- Pisa group: Analytical continuation from imaginary  $\theta$

[D'Elia et al 1306.2919], [Bonati et al 1512.01544, 1607.06360,1807.06558]

*Extract  $\chi$ ,  $b_2$ ,  $dT_c/d\theta^2$ , (+ effect of  $\text{Tr } P = 0$ )*

- Integral method, analogous to equation of state with  $\epsilon - 3p$

Frison et al [1606.07175], Wuppertal [1606.07494]

*Relative weight of  $Q = 0$  and  $Q = 1$  sectors are calculated*

- Darmstadt: Metadynamics with reweighting

[Jahn et al 1805.11511, 2002.01153]

*Metropolis step to enhance dislocations*

- Pisa group: Multicanonical approach

[Bonati et al 1807.07954]

*Topology enhancement term is built into the HMC force*

- Density of states approach

[Gattringer&Orasch 2101.03383], [Borsanyi&Sexty 2101.03383]

*Explore a broad range in  $Q$  with constrained simulations*

$$Z = \int D\Phi e^{-S[\Phi]}.$$

The Gaussian integral  $\int_{-\infty}^{\infty} dc e^{-\frac{P}{2}(c-a)^2} = \sqrt{\frac{2\pi}{P}}$  is  $a$ -independent.

$$Z = \int D\Phi \int_{-\infty}^{\infty} dc e^{-\frac{P}{2}(c-F[\Phi])^2} e^{-S[\Phi]},$$

where  $F[\Phi]$  is an arbitrary functional of the fields. Swapping the order of the integrations we can write

$$Z = \int_{-\infty}^{\infty} dc \rho(c)$$

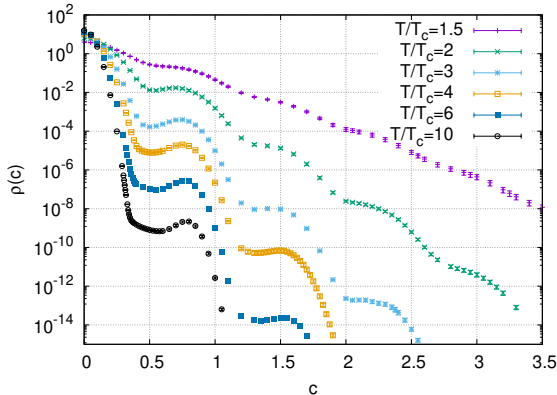
where we defined the  $\rho(c)$  as the 'density of states':

$$\rho(c) = \int D\Phi e^{-S[\Phi] - \frac{P}{2}(c-F[\Phi])^2}.$$

# Density of states method

$\rho(c)$  can be calculated with from a mesh of  $c$ -ensembles:

$$\frac{\partial \ln \rho(c)}{\partial c} = \frac{1}{\rho(c)} \int D\Phi e^{-S[\Phi] - \frac{p}{2}(c - F[\Phi])^2} (-P(c - F[\Phi])) = \langle -P(c - F[\Phi]) \rangle_c,$$



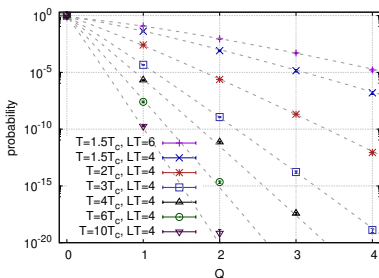
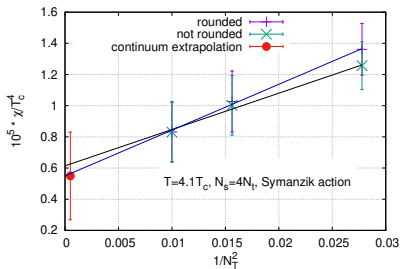
In our work  $F[\Phi]$  is the stout-smearred  $Q_{\text{proxy}} \sim \int \tilde{F} dV$

# Density of states method for the topological charge

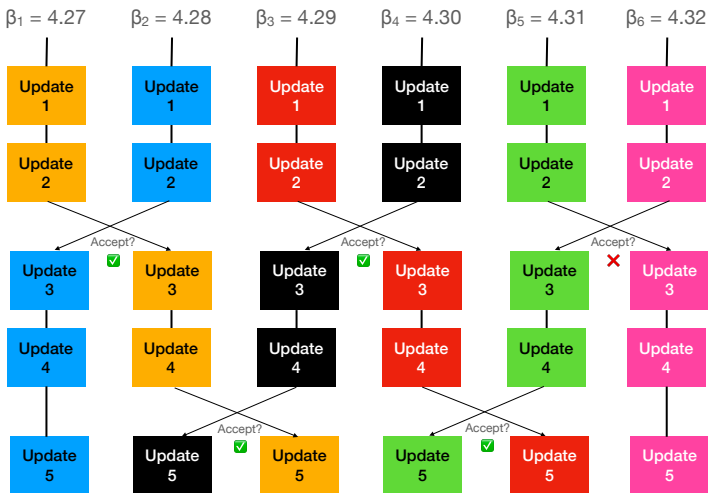
Any observable  $A$  can be then expressed as

$$\langle A \rangle = \frac{1}{Z} \int_{-\infty}^{\infty} dc \int D\Phi A[\Phi] e^{-S[\Phi] - \frac{P}{2}(c - F[\Phi])^2} = \frac{\int_{-\infty}^{\infty} dc \rho(c) \langle A \rangle_c}{\int_{-\infty}^{\infty} dc \rho(c)}$$

*Histogram of  $Q$ :  $h(n) = \int dc \rho(c) \langle \delta_{Q,n} \rangle_c$ .*



# The parallel tempering update



# The tempering Metropolis step

The tempering update fulfills detailed balance with the joint equilibrium distribution:

$$Z = \prod_i Z_i = \prod_i \int DU_i e^{-S_i(U_i)} = \int DU_1 \cdots DU_N e^{-S_1(U_1) \cdots -S_N(U_N)}$$

Swapping ( $a \leftrightarrow b$ ) is accepted with  $P(a, b)$ :

$$P(a, b) e^{-S_a(U_a) - S_b(U_b)} = P(b, a) e^{-S_b(U_a) - S_a(U_b)}$$

The corresponding Metropolis step:

$$P(a, b) = \min(1, e^{-\Delta H})$$

with

$$\Delta H = [S_b(U_a) + S_a(U_b)] - [S_a(U_a) + S_b(U_b)]$$

*Technically:*

*The node holding the  $U_a$  configuration calculates  $S_a(U_a)$  and  $S_b(U_a)$  and communicates to the master. The master works out all swaps.*



# Many uses of parallel tempering

- [Swendsen&Wang Phys.Rev. Lett. 57 (1986) 2607]

## *Replica Monte Carlo simulation of spin-glasses*

Introduce temperature as a new dimension.

- [Marinari&Parisi Europhys. Lett. 19 (1992) 451]

## *Simulated tempering: A New Monte Carlo scheme*

Add dynamics to the temperature parameter.

- [G. Boyd Necl. Phys. Proc. Suppl 60A (1998) 341], [E.-M. Ilgenfritz et al. Phys. Rev. D65 (2002) 094506], [B. Joo et al Phys. Rev. D59 (1999) 114501]

Application to lattice QCD with dynamical fermions ( $\kappa$ )

- [G. Burgio et al. Phys Rev D75 (2007) 014504]

Lattice gauge theory near a phase boundary.

- [M. Hasenbusch et al. Phys.Rev. D96 (2017) 054504]

[C. Bonani et al. JHEP 03 (2021) 111]

Topological freezing  $\rightarrow$  open boundary conditions + tempering

- [Borsanyi&Sexty Phys. Lett. B815 (2021) 136148]

Tempering combined with density of states: **topological charge**

- [R. Kara (Wuppertal) Lattice'21]

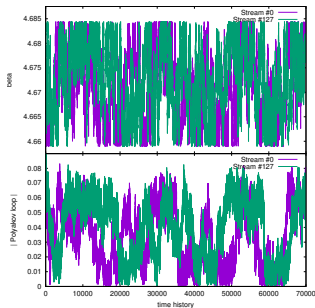
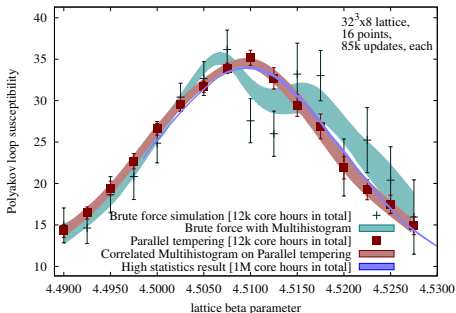
Seaching for the heavy critical mass in the Columbia plot. . .

- [Wuppertal: Phys. Rev. D. 105 (2022) 074513]

**SU(3) Yang Mills theory**

# Parallel tempering: a susceptibility peak

Let us simulate the transition in the SU(3) Yang-Mills theory. The susceptibility of the Polyakov loop exhibits a peak near  $\beta_c$ .

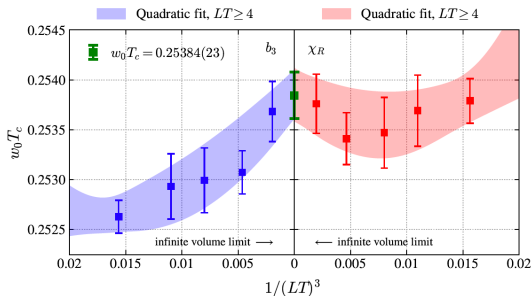


*Tempering updates give the combining effect Ferrenberg&Swendsen's multihistogram reweighting.*

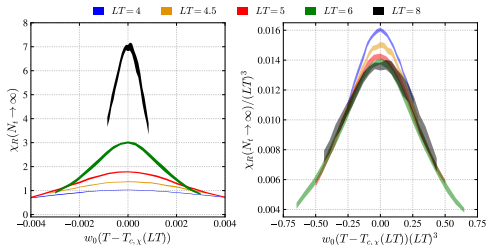
*In addition, the tempering updates allow a stream to thermalized with dynamically changing temperatures.*

# scaling of the Polyakov susceptibility

The continuum extrapolated transition temperature  $w_0 T_c$  scales with  $1/V$ :



The renormalized Polyakov loop susceptibility converges to a scaling curve.



# The order of the transition

In a real transition susceptibilities diverge with the volume  $V$

$$\chi \sim V(\langle O^2 \rangle - \langle O \rangle^2)$$

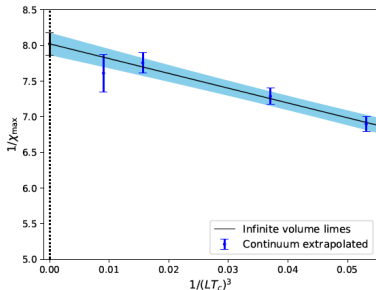
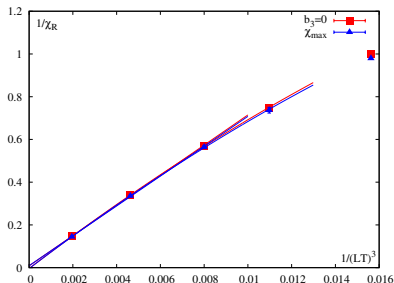
Left) Yang-Mills theory ( $O \equiv$  Polyakov loop)

[Phys. Rev. D. 105 (2022) 074513]

Right) QCD with physical quark masses ( $O \equiv \bar{\psi}\psi$ )

[Nature 443 (2006) 675-678]

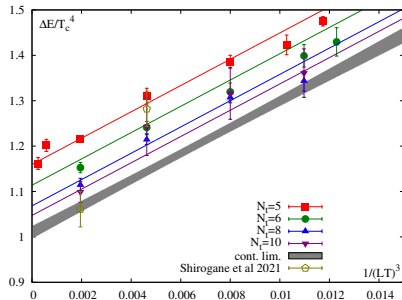
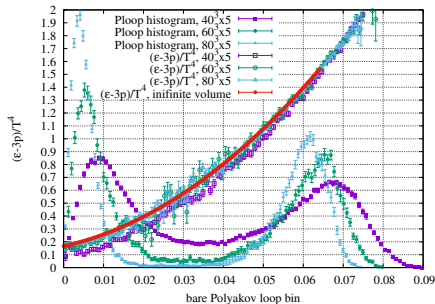
[Phys.Rev.Lett. 125 (2020) 5, 052001]



On both sides: continuum extrapolated results

## Latent heat: the discontinuity of e.g. the trace anomaly

[Svetitsky (1983), Kogut (1983), Gottlieb (1987), Beinlich(1996) Shirogane (2016) and (2020)]



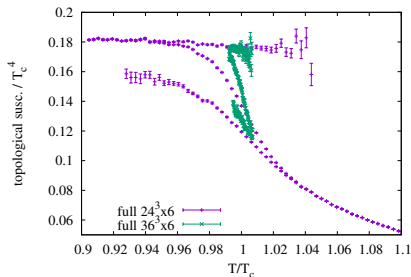
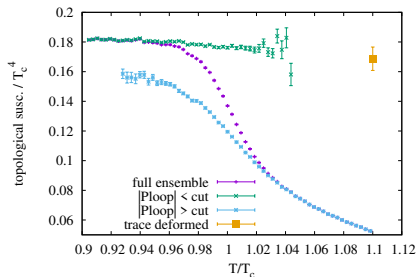
*Observation: The trace anomaly is a continuous function of the Polyakov loop magnitude, and this function can be extrapolated to infinite volume.*

Standard procedure: split the ensemble into two by the Polyakov loop.  
Latent heat is the difference of  $(\epsilon - 3p)/T_c^4$  between the two phases.

$$\frac{\Delta \epsilon}{T_c^4} = \Delta \left[ \frac{\epsilon - 3p}{T^4} \right] = 1.025(21)_{\text{(stat)}}(27)_{\text{(sys)}}$$

# $\chi_t(T)$ near $T_c$ : coexistence of phases

We analyze on the distribution of the topological charge on a toy lattice at  $T_c$ .



[See Bonati et al 1807.06558 for more trace deformed simulations. ]

What follows, the susceptibility has a discontinuity  $\Delta\chi$ . This was, in fact, predicted by a Classius-Clapeyron-like equation [D'Elia&Negro 1205.0538]

$$\frac{T_c(\theta)}{T_c(0)} = 1 - \underbrace{\frac{\Delta\chi}{2\Delta\epsilon}}_{\kappa_\theta} \theta^2 + \mathcal{O}(\theta^4)$$

Continuum limit for the curvature  $\kappa_\theta = 0.0178(5)$  [D'Elia&Negro 1306.2919]

Combined with the latent heat this gives  $\Delta\chi/T_c^4 = 0.0365(18)$ .

Our recent lattice simulations have explored the QCD phase diagram

- Transition line [2002.02821]
- Equation of state using an improved scheme [2102.06660]
- Equation of state with strangeness neutrality [2202.05574]
- with real- $\mu_B$  simulations [2108.09213]

We also use the tool-box to study the  $T - \theta$  phase diagram

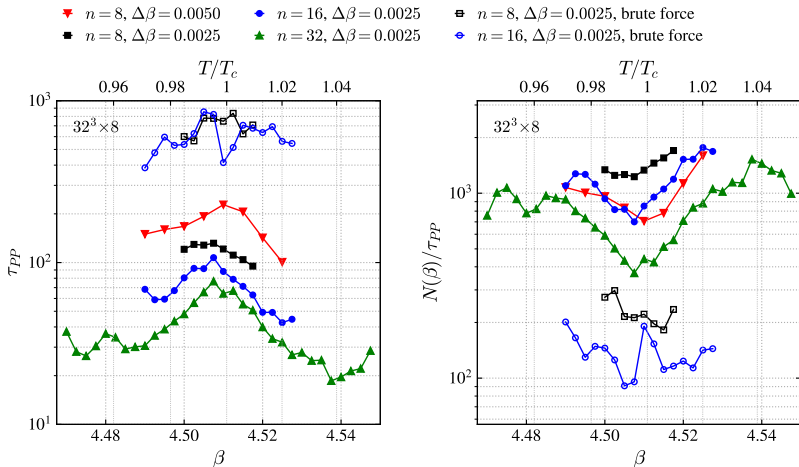
- Density of states [2101.03383]
- Parallel tempering [2202.05234]

For the quenched theory we have new results on  $T_c w_0 = 0.25384(23)$  and the latent heat  $(1.025(21)(27))$ , which implicitly provides  $\Delta\chi = 0.036(2)$ .





# Parallel tempering: autocorrelation times

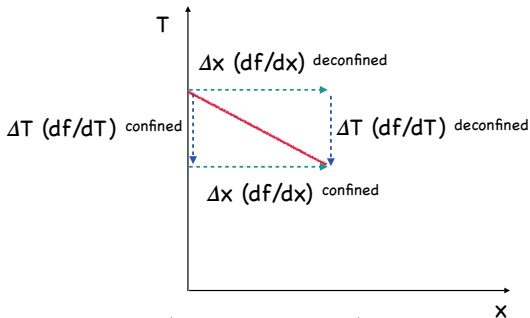


*Runtime: 12000 core hours for each data set*

**Left:** Autocorrelation time

**Right:** Number of updates / autocorrelation time

# On the formula for the $\theta$ -curvature



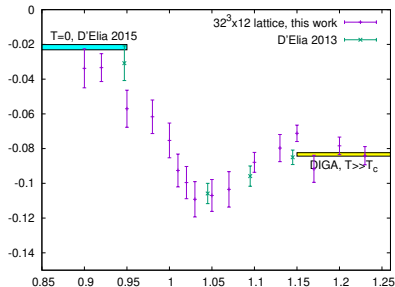
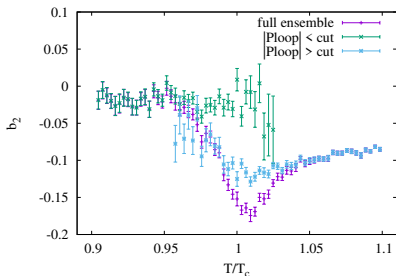
$$\Delta x \left. \frac{df}{dx} \right|_{\text{confined}} + \Delta T \left. \frac{df}{dT} \right|_{\text{confined}} = \Delta x \left. \frac{df}{dx} \right|_{\text{deconfined}} + \Delta T \left. \frac{df}{dT} \right|_{\text{confined}}$$

$$-T \Delta S = \left. \frac{df}{dT} \right|_{\text{deconfined}} - \left. \frac{df}{dT} \right|_{\text{confined}} \quad \frac{1}{2} \Delta \chi = \left. \frac{df}{dx} \right|_{\text{deconfined}} - \left. \frac{df}{dx} \right|_{\text{confined}}$$

$$\kappa = -\frac{\Delta T}{T \Delta x} = \frac{\Delta \chi}{2 \Delta S}$$

# $b_2(T)$ near $T_c$ : coexistence of phases

We analyze on the distribution of the topological charge on a toy lattice at  $T_c$ .

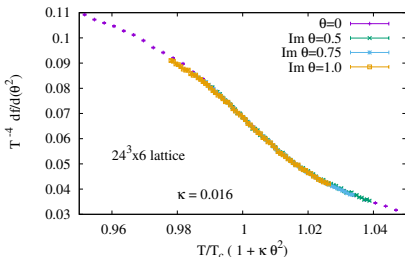
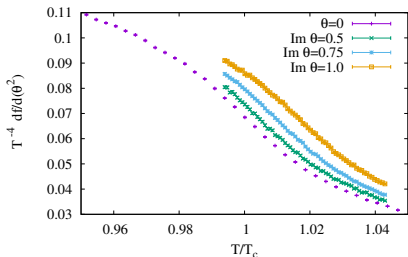


$b_2$  dips below the DIGA limit of  $-1/12$  in the transition region. Phase coexistence drives this to very negative values  $\sim -V$ .

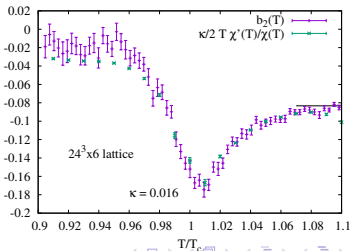
$$b_2 = -\frac{\langle Q^4 \rangle - 3\langle Q^2 \rangle^2}{12\langle Q^2 \rangle} = -\frac{\mathcal{O}(V^2)}{\mathcal{O}(V)}$$

## $b_2(T)$ from the $\kappa_\theta$ curvature

Let us repeat the trick we had in full QCD for  $\chi_1^B(T, \mu_B)$ .  
We analyze the topological charge density at imaginary  $\theta$ .

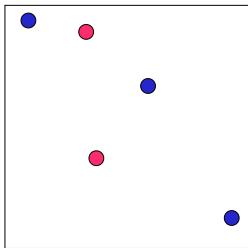


$$b_2 = -\frac{\chi_4}{12\chi_2}$$
$$\kappa(T) = \frac{1}{6T} \frac{\chi_4(T)}{\chi_2'(T)}$$



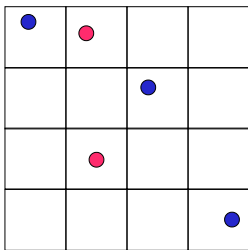
# Axion potential from rare instantons

If instantons are dilute we neglect their interactions.



# Axion potential from rare instantons

If instantons are dilute the universe can be split into sub-volumes.



- Subvolume is small enough: *only one instanton or anti-instanton*

$$Z^{\text{sub}}(\theta) = Z_{Q=-1}e^{-i\theta} + Z_{Q=0} + Z_{Q=+1}e^{+i\theta}$$

- Subvolume is big enough: *large spatial separation:*  
→ no instanton interaction

$$Z(\theta) = \prod_i Z_i^{\text{sub}}(\theta)$$

## Axion potential from rare instantons

If the potential in one volume is

$$V_0^{\text{eff}}(\theta) = -\frac{1}{V_0} \log [Z_0 + Z_{+1} e^{-i\theta} + Z_{-1} e^{i\theta}] , \quad Z_{+1} \stackrel{\text{parity}}{=} Z_{-1} = Z_0 \frac{\chi_t V_0}{2}$$

We can extend this to the whole Universe with  $V_4 = NV_0$ ,  $N \rightarrow \infty$ :

$$V^{\text{eff}}(\theta) = -\frac{1}{V_4} \log [Z_0 + 2Z_1 \cos(\theta)]^N$$

Using  $\chi_t = 2Z_1/Z_0 V_0$  we can write  $2Z_1 = Z_0 \frac{1}{N} V_4 \chi_t$ , thus:

$$V^{\text{eff}}(\theta) = -\frac{1}{V_4} \log \left[ Z_0 + Z_0 \frac{1}{N} V_4 \chi_t \cos \theta \right]^N = -\frac{1}{V_4} \log \left[ 1 + \frac{1}{N} V_4 \chi_t \cos \theta \right]^N + \text{const}$$

In the limit  $N \rightarrow \infty$  we recognize the exponential function:

$$V^{\text{eff}}(\theta) = -\frac{1}{V_4} \log \exp V_4 \chi_t \cos(\theta) + \text{const}$$

$$V^{\text{eff}}(\theta) = \chi(T)(1 - \cos \theta)$$

# Higher moments of the topological susceptibility

The Taylor expansion coefficients of  $V(\theta)$  determine the non-Gaussianity:

$$V(\theta, T) = \frac{1}{2}\chi(T)\theta^2 [1 + b_2(T)\theta^2 + b_4(T)\theta^4 + \dots]$$

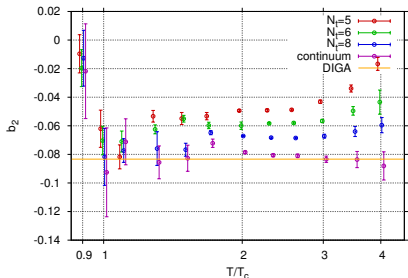
$$b_2 = \frac{\langle Q^4 \rangle - 3\langle Q^2 \rangle^2}{12\langle Q^2 \rangle}$$

If the instanton gas is dilute  $V(\theta, T) \approx \chi(T)(1 - \cos\theta)$

$$b_2 = -1/12, \quad b_4 = 1/360$$

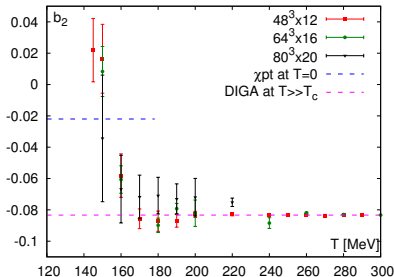
*Chiral perturbation theory:  $b_2 = -0.0022(1)$  (for  $m_u = m_d$ )*

*Yang-Mills theory:*



[Wuppertal-Budapest 1508.06917]

*Full QCD:*



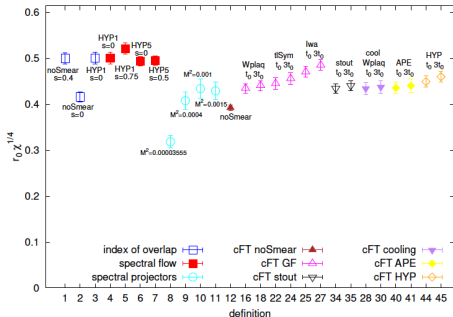
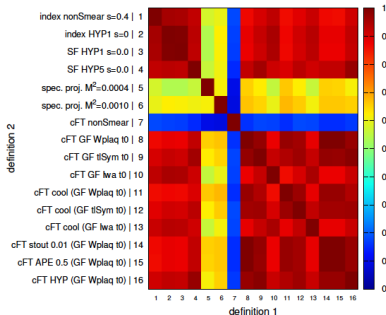
[Wuppertal-Budapest preliminary]

[See also Bonati et al 1512.06746]



# Comparison of many definitions of $Q$

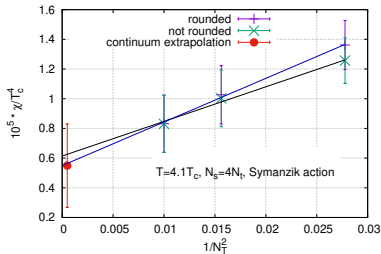
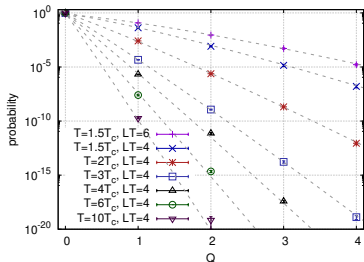
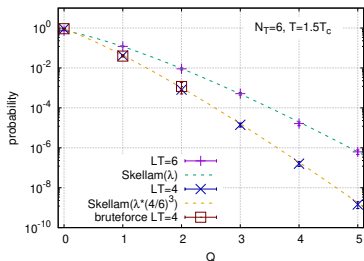
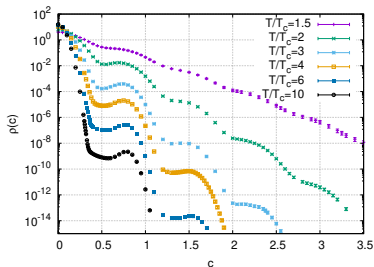
All fermionic and gluonic definitions of the topological charge correlate – except for the unsmeared  $\int G^{\mu\nu} \tilde{G}^{\mu\nu}$ .



The discretization errors can be very different.

[Alexandrou et al 1708.00696]

# DOS results for the distribution of the topological charge



[Borsanyi&Sexty 2101.03383]

*The simulation of  $c$ -mesh was accelerated with parallel tempering.*